300 GHz Channel Characterization of Chip-to-Chip Communication in Metal Enclosure

Jinbang Fu, Juyal Prateek, and Alenka Zajić *Senior Member, IEEE*
Georgia Institute of Technology, Atlanta, GA 30332 USA

***Abstract*—This paper presents the characterization of Terahertz (THz) wireless channel inside a desktop size metal box with focus on line-of-sight (LoS) and reflected-non-line-of-sight (RNloS) propagation. Measurements for LoS propagation inside the metal box show that path loss varies with respect to the transceiver's height from the bottom wall, and for some heights, the path loss is lower than the free space value. By analyzing the relationship between the path loss and the antenna's height, the results show that the first six modes of TE mode dominate the resonating modes inside the box. Also, the path loss analysis indicates that the resonating modes combined with the reflections happened inside the box should be responsible for the strong ripples on the path loss curve. Finally, the RNLoS measurements with dual-in-line-memory-module (DIMM) as the reflecting surface show that the differences between the average path losses measured inside the metal box and in free space are limited to 1 dB.**

***Index Terms*—THz communications, propagation, measurements.**

I. Introduction

Wireless communication has been proposed as a future solution of the chip-to-chip communication inside a desktop for its advantage of reducing the assembly cost of chips and the complexity of system design and maintenance. One limitation of wireless communication is its transmitting data rates. Compared with tens of gigabits per second for wired system, wireless communication can only achieve several gigabits per second [1], [2]. To solve this problem, Terahertz (THz) wireless communication has been proposed for its advantage of providing larger bandwidth and requiring smaller antennas [3].

Channel characterization is the first step to achieve THz chip-to-chip wireless communication inside a desktop. In the microwave frequency range, 3.1-10 GHz, measurements for board-to-board communication have been done inside two desktops, one with crowded interior and the other one with relative empty interior [4]. Also, the chip-to-chip communication has been characterized in both closed and open computer cases in the similar frequency band [5]. At THz frequencies, indoor communication has been conducted for line-of-sight (LoS) propagation by varying distance between transmitter (Tx) and receiver (Rx), and for non-line-of-sight (NLoS) propagation with different transmitting and receiving angles, shadowing effect, and reflection and diffraction from various material [2], [6]–[8]. Additionally, on-board THz wireless communication measurements have been conducted by considering different possible scenarios like LoS, RNLoS, obstructed-line-of-sight (OLoS), and NLoS [2].

This work has been supported, in part, by NSF grant 1651273. The views and findings in this paper are those of the authors and do not necessarily reflect the views of NSF.

For more practical scenario, which involves data communication inside a computer desktop, this paper presents the characterization of 300 GHz wireless channel inside a desktop size metal box. Here, we have focused on the scenarios of LoS propagation with the variation of transceiver's height, h, and RNLoS propagation with Tx and Rx positioned perpendicular with each other. We have analyzed path loss in these two scenarios and the results indicate that both traveling wave and the resonating modes contribute to the received power. By analyzing the relationship between the path loss and the antenna's height, the results show that the first six modes of TE mode dominate the resonating modes inside the box. Also, the path loss analysis indicates that the resonating modes combined with the reflections happened inside the box should be responsible for the strong ripples on the path loss curve. In addition, the RNLoS measurements with dual-in-line-memory-module (DIMM) as the reflecting surface show that the differences between the average path loss measured inside the metal box and in free space are limited to 1 dB.

The remainder of the paper is organized as follows. Section II briefly describes measurement equipment and setup, while Section III describes measurement scenarios. Section IV presents measured results, pathloss modeling and discusses the findings. Section V provides concluding remarks.

II. Measurement Setup

The measurement setup includes the N5224A PNA vector network analyzer (VNA), the VDI transmitter (Tx210) and the VDI receiver (Rx148). The VNA provides the input signal with the range of 10 MHz to 20 GHz. The VDI transmitter amplifies and converts the signal to 300 GHz. The THz signal is transmitted by diagonal horn antenna in the range of 280 to 320 GHz. At the Rx side, the VDI receiver downconverts the received signal to an intermediate frequency (IF) of 9.6 GHz. The VNA records the upper-side of down converted signal in the range of 9.6 to 29.6 GHz. The antenna gain varies between 22-23 dBi over the frequency band of observation, which is 300-312 GHz. The theoretical half power beamwidths (HPBW) are 12°in azimuth and elevation. The physical dimension of the horn aperture is 9.15 mm, which limits the far-field boundary to be 4.23 cm at 300 GHz.

III. Measurement Scenarios

A. LoS Inside a Computer Desktop Size Metal Box

To develop THz wireless communication schemes for chip-to-chip communications, it is necessary first to understand its propagation mechanisms inside an empty metal box. A desktop size aluminum box was built with the size of 30.5 cm$\times$ 30.5 cm$\times$ 10 cm, which approximates computer desktop casing. As shown in Fig. 1, two square aluminum plates with the length of 30.5 cm were fixed by foams at each corner to form the ceil and floor of the metal box. The other four sides of the metal box were covered by aluminum foils. These side walls are labeled as A, B, C, and D as shown in Fig. 1. Box was sandwiched in the middle of Tx and Rx with antennas aligned horizontally. Based on the antenna's height, h, two diagonal openings with the horn antenna's size were drilled on the transceiver sides (side A and side C) of the metal box. The distance from the center of antennas to side B of the metal box is equal to half of its width. To characterize the resonant modes inside the metal box, measurements have performed with h varied from 0 cm to 6.6 cm with the step size of 0.6 cm. The parameter h here refers to the distance between the bottom edge of the horn to the ground of the metal box. The distance between phase center and bottom edge of the horn antenna is 4.575 mm. Absorbers were used to eliminate reflections from the backsides of antennas as shown in Fig. 1.

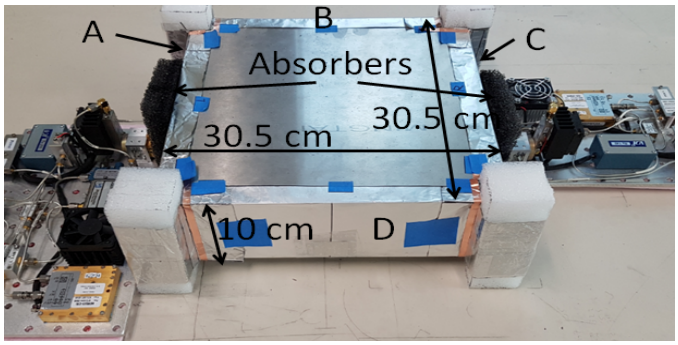

Fig. 1. LoS measurement setup for THz wireless communication in an empty metal box.

B. RNLoS With and Without Memory Card as the Reflecting Surface

Dual in-line memory modules (DIMM) are commonly seen being vertically plugged on the motherboard of a computer. Measurements have been performed both in free space and inside the metal box to study whether DIMM can be used as a reflector to establish a wireless link between the Tx and Rx positioned orthogonal to each other. Fig. 2 shows the measurement setup. As shown in Fig. 2a, a memory was vertically put on the center of the bottom of the box along its diagonal. Tx and Rx are positioned on the side A and D, respectively, as shown in Fig. 2b. For the in-box measurements, two diagonal openings were drilled on side A and side D of the box for the horn antennas. Both, flat side and component side of the DIMM were measured with $h = 2.4$ cm. The scenario without DIMM between transceivers also has been measured.

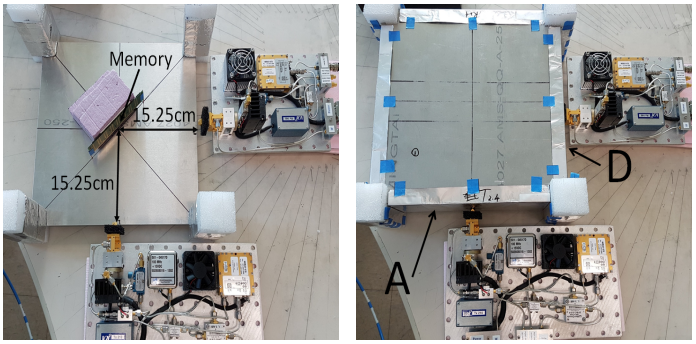

(a) (b)

Fig. 2. RNLoS measurements setups for (a) free space and (b) in-box measurements with/without DIMM as the reflecting surface.

IV. Measurement Results and Analysis

A. Definitions of Path Loss and Multipath Propagation

This section analyzes and discusses results of the measurements described in previous section. Here, PL is used to represent the measured path loss, and is defined as

$$PL = \frac{P_t G_t G_r}{P_r}, \tag{1}$$

where P_t represents the transmit power, G_t and G_r are the transmit and receive gain of the antenna being used, and P_r is the received power. The measured path loss was compared with the theoretical free-space path loss defined as [9]

$$\tilde{PL} = \left(\frac{4\pi d}{\lambda}\right)^2, \tag{2}$$

where d represents the distance between the Tx and Rx, and λ is the wave length is free space.

For the measurements performed inside the metal box, resonant modes should be taken into consideration. The transverse components of the electric field ($E_z = 0$) of TE mode inside the cavity can be written as [10]

$$E_y = \frac{j\omega_{mnp}\mu k_x H_0}{k_{mnp}^2 - k_z^2} \sin\frac{m\pi x}{a} \cos\frac{n\pi y}{b} \sin\frac{p\pi z}{z}, \tag{3}$$

$$E_x = -\frac{j\omega_{mnp}\mu k_y H_0}{k_{mnp}^2 - k_z^2} \cos\frac{m\pi x}{a} \sin\frac{n\pi y}{b} \sin\frac{p\pi z}{z}, \tag{4}$$

where H_0 is an arbitrary constant with units of A/m and m, n, and p are integers. The eigenvalues k_{mnp} satisfy:

$$k_{mnp}^2 = \left(\frac{m\pi}{a}\right)^2 + \left(\frac{n\pi}{b}\right)^2 + \left(\frac{p\pi}{c}\right)^2 = k_x^2 + k_y^2 + k_z^2, \tag{5}$$

where

$$k_x = \frac{m\pi}{a}, k_y = \frac{n\pi}{b}, k_z = \frac{p\pi}{c}. \tag{6}$$

a, b, and c in these equations represent the height, length, and width of the cavity as shown in Fig. 3. The resonant frequencies f_{mnp} can be determined as

$$f_{mnp} = \frac{1}{2\sqrt{\mu\epsilon}} \sqrt{\left(\frac{m}{a}\right)^2 + \left(\frac{n}{b}\right)^2 + \left(\frac{p}{c}\right)^2} \tag{7}$$

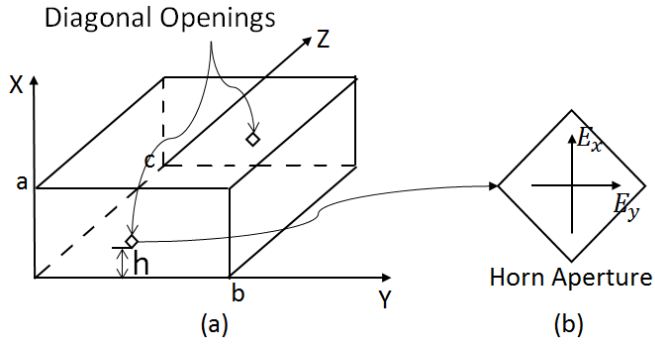

Fig. 3. (a) Rectangular metal cavity with diagonal openings and (b) the horn antenna aperture.

The impulse response for the time-invariant channel can be written as [11]

$$h(\tau, d) = \sum_{k=1}^{L} a_k(d) exp(j\theta_k(d))\delta(\tau - \tau_k), \tag{8}$$

where d represents the distance between the Tx and Rx, L represents the number of multipath components, a_k represents the amplitude of the k^{th} multipath component, θ_k is the associated phase, and τ_k represents the excess delay of the k^{th} path compared with the first one, and $\delta(\cdot)$ is the Dirac delta function. The equations for the mean excess delay, τ_m, the RMS delay spread, τ_{rms}, and the coherence bandwidth, B_c, of the channel can be written as [11]

$$\tau_m = \sum_{k=1}^{L} \tau_k \cdot |h(t, \tau_k, d)|^2, \tag{9}$$

$$\tau_{rms} = \sqrt{\sum_{k=1}^{L} (\tau_k - \tau_m)^2 |h(t, \tau_k, d)|^2}, \tag{10}$$

$$B_c = \frac{1}{2\pi\tau_{rms}}, \tag{11}$$

where L is the number of multipath components, and τ_k represents excess delay of the k_{th} path.

B. Characterization of LoS Propagation Inside a Metal Box

Section III-A describes the measurement scenario for exploring the signal propagation mechanisms inside an empty metal box. The scenario is shown in Fig. 2. Fig. 4 shows the measured path losses for in the box measurements and compares them with theoretical path loss calculated using Friis formula. For the measurements with $h < 1.8$ cm, path losses are lower than Friis formula prediction, while for $h > 1.8$ cm, path losses are aligned with the Friis formula prediction. This variation of path losses can be explained by observing that different resonant modes contribute to the received power. We note here that since transmit power is kept constant, the variation in the path loss is equal to the variation of the received power. To show this, the measured received power/path loss variation with respect to h is shown in Fig. 5 and compared with the theoretically calculated power variation. Path losses

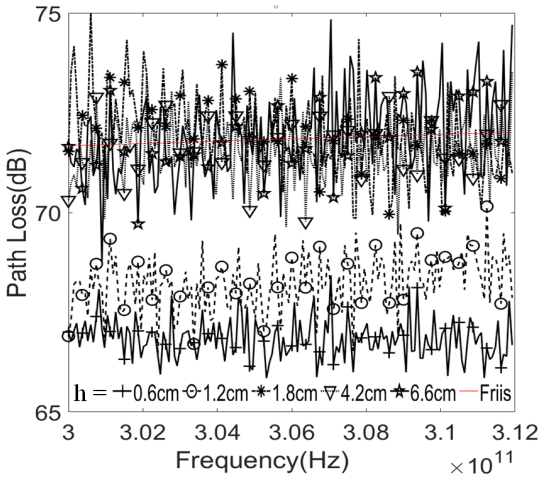

Fig. 4. Measured and calculated path loss variation in frequency for LoS in a metal box as a function of the antenna's height, h.

are averaged over all recorded frequencies. To represent the path loss variation, average path losses are normalized with the maximum value which is 71.93 dB. The measured received variation curve shown in Fig. 5 is the interpolation of these normalized points which are also marked on the curve.

The calculated received power variation in Fig. 5 is obtained by modeling resonant modes in the metal box. For a given frequency, the received power contributed by the resonant modes inside the box (P_R) can be written as the summation of the power contributed by individual modes (P_1,P_2,$\cdots$,P_n), i.e.,

$$P_R = \sum_{n=1}^{l} P_n = \sum_{n=1}^{l} (E_{yn}^2 + E_{xn}^2), \tag{12}$$

where l is an integer greater or equal to 1. The expression for E_{yn} and E_{xn} are given by equations (3) and (4), respectively. Since only h varied in the x direction shown in Fig. 3, the equations (3) and (4) can be simplified as follows

$$E_{ym} = A_m \sin\frac{m\pi x}{b}, \tag{13}$$

$$E_{xm} = B_m \cos\frac{m\pi x}{a}. \tag{14}$$

Then, P_R can be written as

$$P_R = \left(A_n \sin\frac{n\pi x}{b}\right)^2 + \left(B_n \cos\frac{n\pi x}{a}\right)^2. \tag{15}$$

Using curve-fitting, we have found that the first 6 modes dominate the resonant cavity in the box and the coefficients of these modes are empirically found to be $A_1 = 0.832, B_1 = 0.022, A_2 = 0.519, B_2 = 0.044, A_3 = 0.065, B_3 = 0.297, A_4 = 0.013, B_4 = 0.470, A_5 = 0.039, B_5 = 0.146, A_6 = 0.327, B_6 = 0.125$.

Fig. 6 presents the PDP of the empty box measurements for different h values. After the first arriving peak, there are several clusters of peaks that arrive with delay of 2.05 ns. This delay is due to the signal traveling on a certain path

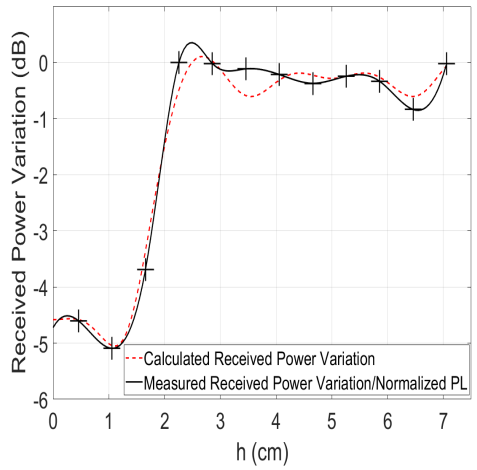

Fig. 5. Measured and calculated received power variation as a function of antenna hight h.

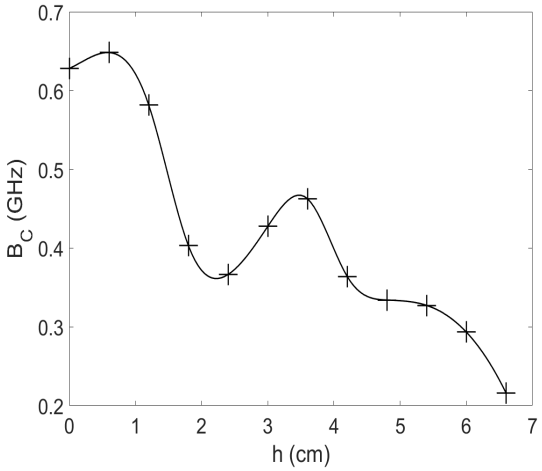

Fig. 7. Coherence bandwidth, B_c, as a function of antenna height h, for the channel inside a metal box.

many times and the path difference between any two close paths can be calculated as

$$T \times c = 2.05 \times 10^{-9} \cdot 3 \times 10^{8} = 61.5 \text{ cm}, \qquad (16)$$

which is close to twice of the box's length. Therefore, it can be concluded that the signal bounces several rounds between the transceiver sides (side A and C) of the box. This is due to the traveling wave inside the box. Fig. 7 shows the coherence

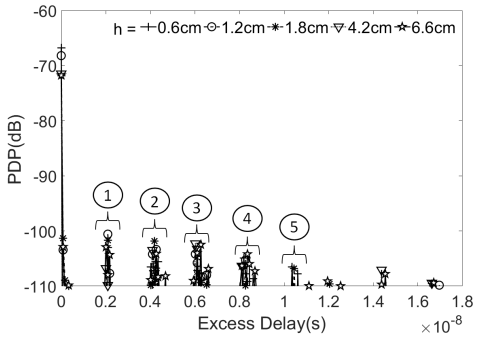

Fig. 6. Power delay profile of the metal box measurements shown in the Fig. 1 as a function of antenna height h.

bandwidth B_c as a function of the antenna height h. Due to the traveling wave bouncing back and forth between the transceiver sides of the box, the B_cs of channel inside the empty box is below 1 GHz. This is due to the introduced multipath. It can be observed from Fig. 7, the B_c has larger values closer to the bottom wall as compared to the antenna height $h > 4$ cm.

C. Characterization of RNLoS Inside a Metal Box

Fig. 8 compares the path losses of RNLoS link measured both in free space and inside the box. Measurement setup is shown in Fig. 2 of section III-B. Measured path losses are shown when DIMM component rough and flat side are used as reflecting surfaces, respectively. For comparison, we also plot the path loss for the scenario without DIMM between the transceivers. Fig. 8a compares the path loss measured in free space with Friis formula. Due to the reflection losses, the path losses for both flat and rough side of the DIMM are greater than the Friis formula prediction. The path loss of the rough side of DIMM is greater than the path loss of the flat side of DIMM, which is expected as the rough DIMM side is more rugged than the flat side of DIMM. In case of the scenario without DIMM between transceivers, the measured pathloss is near noise floor which indicates no communication between Tx and Rx. This is also observed in [8]. Fig. 8b shows the measurements inside the box. It is found that for both rough and flat side of the DIMM as the reflecting surfaces, the path loss measured in the metal box is at the similar level of the path loss measured in the free space with the differences of average path loss limited to 1 dB. However, it is interesting to notice that curves shown Fig. 8a have stronger ripples than curves in Fig. 8b. This is due to the effect of resonant modes in the metal box. Furthermore, the path loss for the measurement without DIMM between the transceivers is shown in Fig. 8b. In contrast to the free space, this path loss is not close to the noise floor and is due to the resonant modes that exist in the box.

Fig. 9 shows the power delay profiles (PDP) of the RNLoS link for the in-box measurements. From the PDP plot, it can be observed that there are two later arriving peaks that are result of reflections from both rough and flat DIMM side. For the flat side of DIMM, those two later arriving peaks are located at 2.05 ns and 4.09 ns, respectively. These two later arriving peaks illustrate that with the help of the DIMM, the signal can travel several rounds between the transceiver sides (side A and D) of the box. For the rough DIMM side, those two later arriving peaks are at 1.17 ns and 2.05 ns, respectively. This shows that signal also bounced back and forth between the DIMM and the transceiver.

Table I shows τ_m , τ_{rms}, and B_c of the RNLoS link for the measurements performed inside the box. When comparing

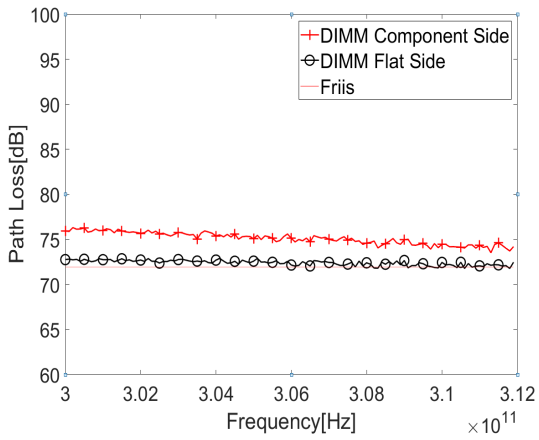

(a)

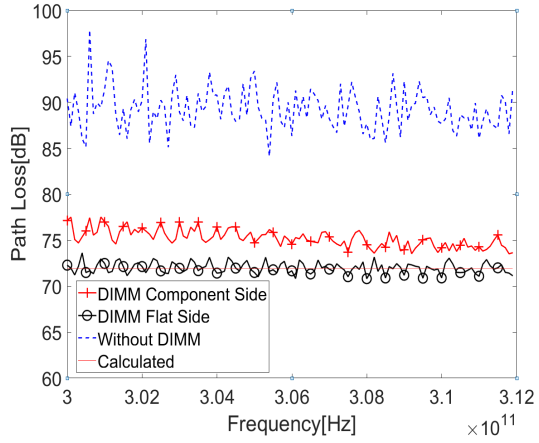

(b)

Fig. 8. Measured and calculated path losses of RNLoS with rough DIMM side, flat DIMM side, and without DIMM as the reflecting surface for the measurements (a) in free space and (b) inside the box.

with the PDP plot of the empty box measurements, the in-box RNLoS link has less later arriving peaks, which provides the channel a much wider B_c. From Fig. 9, it can be observed that the later arriving peaks' amplitudes of the rough side DIMM are lower than the later arriving peaks' amplitudes of the flat side DIMM, which indicates that comparing with the DIMM flat side, the channel constructed with the rough side of DIMM as the reflecting surface can achieve a wider B_c. DIMM can be utilized to help construct the wireless link when the Tx and Rx are in perpendicular with each other.

TABLE I
τ_m, τ_{rms}, AND B_c OF RNLOS LINK FOR MEASUREMENTS INSIDE THE BOX

Measurements	τ_m (ps)	τ_{rms} (ns)	B_c (GHz)
DIMM Flat Side	4.971	0.1251	1.273
DIMM Component Side	2.217	0.0618	2.576
Without DIMM	-	-	-

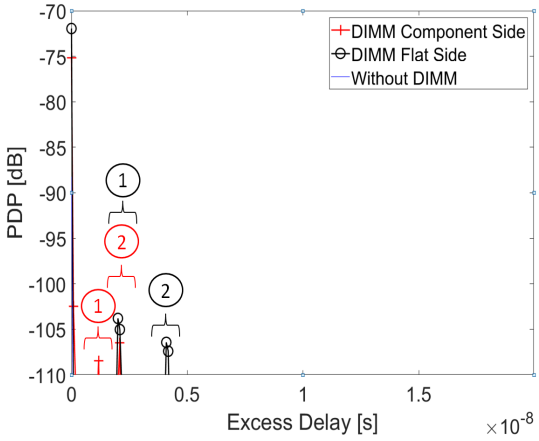

Fig. 9. PDP of RNLoS link with rough side DIMM, flat side DIMM, and without DIMM as the reflecting surface for in-box measurements.

V. Conclusions

This paper presents the characterization of THz wireless channel inside a metal box. We have found that both traveling wave and resonant modes exist inside the box. With the analysis of LoS propagation inside the metal box, it is found that the received power variation with respect to the antenna's height is due to the resonant modes dominated by first 6 TE modes inside the metal box. The multipath introduced by traveling wave limits the coherence bandwidths. Finally, for RNLoS propagation inside the metal box, traveling wave dominates the channel, and the stronger ripples of path losses over frequency band are due to resonant modes that exist in the box.

References

[1] S. Khademi, S. P. Chepuri, Z. Irahhauten, G. J. Janssen, and A.-J. van der Veen, "Channel measurements and modeling for a 60 ghz wireless link within a metal cabinet," *IEEE Trans. Wireless Communications*, vol. 14, no. 9, pp. 5098–5110, 2015.

[2] S. Kim and A. Zajić, "Characterization of 300-ghz wireless channel on a computer motherboard," *IEEE Transactions on Antennas and Propagation*, vol. 64, no. 12, pp. 5411–5423, 2016.

[3] P. H. Siegel, "Terahertz technology," *IEEE Transactions on microwave theory and techniques*, vol. 50, no. 3, pp. 910–928, 2002.

[4] J. Karedal, A. P. Singh, F. Tufvesson, and A. F. Molisch, "Characterization of a computer board-to-board ultra-wideband channel," *IEEE Communications letters*, vol. 11, no. 6, 2007.

[5] Z. Chen and Y. P. Zhang, "Inter-chip wireless communication channel: Measurement, characterization, and modeling," 2007.

[6] N. Khalid and O. B. Akan, "Wideband thz communication channel measurements for 5g indoor wireless networks," in *Communications (ICC), 2016 IEEE International Conference on*. IEEE, 2016, pp. 1–6.

[7] S. Priebe, C. Jastrow, M. Jacob, T. Kleine-Ostmann, T. Schrader, and T. Kurner, "Channel and propagation measurements at 300 ghz," *IEEE Transactions on Antennas and Propagation*, vol. 59, no. 5, pp. 1688–1698, 2011.

[8] S. Kim and A. G. Zajić, "Statistical characterization of 300-ghz propagation on a desktop," *IEEE Transactions on Vehicular Technology*, vol. 64, no. 8, pp. 3330–3338, 2015.

[9] H. T. Friis, "A note on a simple transmission formula," *Proceedings of the IRE*, vol. 34, no. 5, pp. 254–256, 1946.

[10] D. A. Hill, *Electromagnetic fields in cavities: deterministic and statistical theories*. John Wiley & Sons, 2009, vol. 35.

[11] A. Zajic, *Mobile-to-Mobile Wireless Channels*. Norwood, MA, USA: Artech House, Inc., 2013.